Medicine®

OBSERVATIONAL STUDY

OPEN

Desmoid-Type Fibromatosis of the Thorax: CT, MRI, and FDG PET Characteristics in a Large Series From a Tertiary Referral Center

Hai Xu, MD, Hyun Jung Koo, MD, PhD, Soyeoun Lim, MD, Jae Wook Lee, MD, Han Na Lee, MD, Dong Kwan Kim, MD, PhD, Joon Seon Song, MD, PhD, and Mi Young Kim, MD, PhD

Abstract: The purpose of this study was to describe the radiologic findings of computed tomography (CT), magnetic resonance (MR) imaging, and ^{18}F-fluorodeoxy glucose positron emission tomography (FDG PET) in desmoid-type fibromatosis of the thorax.

We retrospectively evaluated 47 consecutive patients with pathologically proven desmoid-type fibromatosis from January 2005 to March 2015. Patients underwent CT (n = 36) and/or MR (n = 32), and 13 patients also underwent FDG PET. Based on CT and MR, the sizes, locations, margins, contours, presence of surrounding fat, extra-compartment extension, bone involvement, and neurovascular involvement of the tumors were recorded. The attenuation, signal intensity, enhancement pattern, and presence of internal low signal band or signal void of the tumors were evaluated. Initial image findings were then compared between 2 groups of tumors: group 1 with recurrence or progression, and group 2 with no recurrence or stable without treatment.

Median age at diagnosis of the tumors was 45 years, range 4 to 96, female-to-male ratio 1.8. Median tumor long diameter was 65 mm (range, 22–126 mm). The most common locations were chest wall (42.6%), followed by supraclavicular area, shoulder or axillary area, and mediastinum. The tumors had well-defined margins (83.0%), lobulated in contours (66.0%) surrounding fat (63.8%), extra-compartment extensions (42.6%), bone involvements (42.6%), and neurovascular involvements (27.7%). On CT, tumors had low attenuation (60.0%) with mild enhancement (median 24 HU, range 0–52). On MR, they showed iso-signal intensity (SI) (96.9%) on T1-weighted images (WI), and high SI (90.6%) on T2WI images, with strong (87.5%) and heterogeneous (96.9%) enhancement. Internal low signal bands (84.4%) and signal voids (68.8%) were noted. The median value of maxSUV was 3.1 (range, 2.0–7.3). In group 1 (n = 19, 40.4%), 13 patients suffered recurrence and 6 experienced progression. Group 2 (n = 28, 59.6%) consisted of 21 patients with no recurrence and 7 stable patients receiving no treatment. Partially ill-defined margins (OR, 0.167; 95% CI 0.029–0.943; $P = 0.043$) was the independent predictor for recurrence or progression of tumor.

Knowledge of the radiological findings in desmoid-type fibromatosis on CT, MR, and FDG PET may help to improve diagnosis. Tumors with partially ill-defined margins have a tendency to recur or progress.

(*Medicine* 94(38):e1547)

Abbreviations: CT = computed tomography, FDG PET = ^{18}F-fluorodeoxy glucose positron emission tomography, maxSUV = maximum standardized uptake value, MR = magnetic resonance.

INTRODUCTION

Desmoid-type fibromatosis is a benign, deep-seated monoclonal myofibroblastic neoplasm that arises from musculoaponeurotic stromal elements and grows slowly with a tendency to infiltrate. Recently, the term ''aggressive fibromatosis'' or ''desmoid tumor'' has also come into use. The word ''desmoid'' originates from the Greek, and means tendon-like or band-like.[1] In the 2002 World Health Organization classification of soft tissue tumors, desmoid-type fibromatosis is classified as an ''intermediate'' tumor, one that is locally aggressive but never metastasizes.[2]

Desmoid-type fibromatosis is rare, it accounts for approximately 0.03% of all neoplasms and less than 3% of all soft tissue tumors. It can occur in any anatomic location, and its incidence in the general population is estimated at about 2 to 4 per million per year.[3–5]

Apart from a limited number of radiologic reports,[6] previous descriptions of desmoid-type fibromatosis of the thorax have mostly focused on their clinical and pathologic features; imaging features were not the major concern and were often equivocally described.[7,8] Although there have been a few radiologic reports of desmoid-type fibromatosis, they lacked details that could be of use in differentiating desmoid-type fibromatosis from other masses in the thorax.[9,10] In addition, few studies included the use of ^{18}F-fluorodeoxyglucose positron emission tomography (FDG PET).[11,12]

In the present work, we investigated the relation between the image features and pathologic features of desmoid-type fibromatosis in the thorax. Our aim was to establish the detailed clinical, computed tomography (CT), magnetic resonance (MR) imaging, and FDG PET characteristics of desmoid-type fibromatosis using a large confirmed dataset in a tertiary referral center, and to investigate the long-term follow-ups.

Editor: Jianfeng Li.
Received: June 12, 2015; revised: August 12, 2015; accepted: August 18, 2015.
From the Department of Radiology and Research Institute of Radiology, University of Ulsan College of Medicine, Asan Medical Center, Seoul, Korea (HX, HJK, SL, JWL, HNL, MYK); Department of Radiology, The First Affiliated Hospital of Nanjing Medical University, Nanjing, Jiangsu Province, China (HX); Department of Thoracic and Cardiovascular Surgery (DKK); and Pathology, University of Ulsan College of Medicine, Asan Medical Center, Seoul, Korea (JSS).
Correspondence: Mi Young Kim, Department of Radiology and Research Institute of Radiology, University of Ulsan College of Medicine, Asan Medical Center, Seoul, Korea (e-mail: mimowdr@gmail.com).
HX and HJK contributed equally to this work.
The authors have no funding and conflicts of interest to disclose.

ISSN: 0025-7974
DOI: 10.1097/MD.0000000000001547

MATERIALS AND METHODS

Patient Characteristics

This study conducted at a single, tertiary center was approved by our Institutional Review Board (Approval number: S2015–0544), and informed consent was waived. We searched our pathological database using the keywords desmoid OR fibromatosis, from January 2005 to March 2015, and finally found 199 pathologically proven cases of desmoid-type fibromatosis. Of the 199 cases, 148 were excluded because of extrathoracic location of the tumors, and a further 4 patients without CT and MR images were also excluded. Finally, 47 consecutive patients were included in the study (Figure 1). All 47 patients underwent CT (n = 36) and/or MR (n = 32), and 13 of them also underwent FDG PET. The interval between CT and MR was less than 1 month except in 3 patients, and the median interval was 20 days (interquartile range [IQR], 13–28). The intervals between CT, MR, and PDG PET were less than 1 month except for 4 patients, and the median interval was 16 days (IQR, 6–38).

Information regarding clinical symptoms, pathologic results, and treatment methods was obtained from an electronic medical chart. Tumor recurrence, progression, and disease-specific survival rates were evaluated by reviewing the medical records up to the latest visit to the outpatients' clinic. We divided the patients into group 1 (recurrence or progression despite treatment) and group 2 (no recurrence after treatment or no treatment due to stability), and then compared the clinical and initial image findings between the 2 groups.

Diagnosis of Desmoid-Type Fibromatosis

Tissue Confirmation by Core Needle Biopsy

Of the 47 patients, 41 (87.2%) were pathologically confirmed by fluoroscopy or CT-guided core-needle biopsy (Table 1). CT-guided core needle biopsies were performed with a 16-channel CT SOMATOM Sensation (Siemens Medical Solutions, Forchheim, Germany), and fluoroscopy-guided core needle biopsies were performed using a Siemens Artis zee multipurpose system (Siemens AG, Muenchen, Germany). All procedures were performed by expert chest radiologists with an 18- or 20-gauge semiautomatic core biopsy needle (Stericut with coaxial guide, TSK Stericut; TSK Laboratory, Soja, Japan). Two or 3 biopsies were performed at each procedure in order to obtain sufficient specimen for diagnosis.

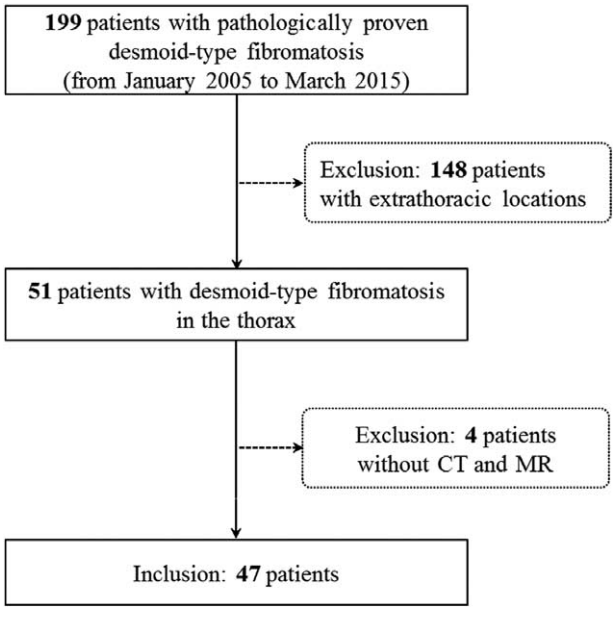

FIGURE 1. Flow chart of patient selection.

Tissue Confirmation by Operation

Thirty five patients (74.5%) were finally confirmed by operation. Among these, 29 had also undergone prior core needle biopsy (Table 1).

TABLE 1. Clinical Characteristics of 47 Patients with Desmoid-type Fibromatosis

Characteristic, n = 47	Median (Range) or Number (%)
Age (median, range)	45 (4–96)
Gender	
Female	30 (63.8)
Male	17 (36.2)
Chief complaint	
Palpable mass	21 (44.7)
Pain	11 (23.4)
No symptom	10 (21.3)
Others*	5 (10.6)
Imaging Modalities	
CT	11 (23.4)
MR	9 (19.1)
CT + MR	14 (29.8)
CT + PET	4 (8.5)
MR + PET	2 (4.3)
CT + MR + PET	7 (14.9)
Tissue Confirmation	
Biopsy	12 (25.5)
Operation	6 (12.8)
Biopsy + Operation	29 (61.7)
Treatment	
Operation	20 (42.6)
CTx	5 (10.6)
Operation + RT	10 (21.3)
Operation + CTx	2 (4.3)
RT + CTx	0 (0.0)
Operation + RT + CTx	3 (6.4)
No treatment	7 (14.9)
Recurrence or progression after Tx	19 (47.5)

CTx = chemotherapy, FDG PET = ^{18}F-fluorodeoxyglucose positron emission tomography, RT = radiotherapy, Tx = treatment, numbers are numbers of patients, and numbers in parentheses are percentages or range.

*Others = chest discomfort, weakness, hoarseness.

CT, MR, and FDG PET Evaluation

CT Scanning Protocol

Chest CT scans were performed using either a 16 channel SOMATOM Sensation (Siemens Medical Solutions, Forchheim, Germany) or a 64 channel LightSpeed Volume Computed Tomography Scanner (General Electric Medical Systems, Milwaukee, WI). The 16-detector row scanner was used with the following parameters: 120 kV peak, 100 effective mAs with dose modulation. The reconstruction intervals for the images were 3- or 5-mm thickness at 3- or 5-mm intervals without gaps (B50 algorithm), and 1-mm reconstructions with 5-mm gaps (B60 algorithm). The 64-detector row scanner was used with parameters of 120 kV peak and 100 to 300 mA with dose modulation. Reconstruction intervals were 5-mm thickness at 2.5- or 5-mm intervals without gaps (lung algorithm), and 2.5- or 1.25-mm reconstructions with 5-mm gaps (bone algorithm). After administration of 100 mL iopromide (Ultravist 300 mg I/mL, Bayer Pharma, Berlin, Germany) and 50 mL of normal saline at a rate of 2.5 mL/sec intravenously using a power injector, enhanced CT images were obtained with a 50 seconds delay. All images were viewed on the mediastinal window (level, 50 Hounsfield units [HU]; width, 450 HU) and lung window (level, −700 HU; width, 1500 HU) axial image settings using a picture archiving and communication system.

MRI Scanning Protocol

MR images were obtained using a 1.5T unit (Avanto; Siemens Medical Solutions, Forchheim, Germany and Achieva; Philips Medical Systems, The Netherlands). The imaging protocol included a precontrast MR examination for optimal localization, and delineation of the tumor using 8 mm axial/coronal T1- and T2-weighted images (WI). Each patient also underwent MR after intravenous administration of Gadolinium contrast material.

CT and MR Evaluation

Two radiologists (MYK and HX; with 18 and 2 years, respectively, of clinical experience in thoracic radiology), who were blind to the clinical data except for the diagnosis of desmoid-type fibromatosis, evaluated the CT images in consensus. Using the CT and MR scans of the 47 patients, we determined the following: sizes (long and short-axis diameters, respectively); locations (chest wall, supraclavicular area, shoulder or axilla, and mediastinum); margins (well-defined and partially ill-defined); contours, (lobulated, circumscribed, and irregular); presence/absence of a rim of surrounding fat, extra-compartment extension, bone involvement, and neurovascular involvement, of the desmoid-type fibromatosis.

For the 36 patients undergoing CT scans, CT features were analyzed as follows: relative attenuations (low-, iso-, and high) compared to the surrounding muscle on pre-enhanced CT (n = 25), enhancement pattern (homogeneous or heterogeneous) (n = 35), and degree of enhancement using attenuation values measured in HU over a circular region of interest (covering much of the lesion) (n = 23).

For the 32 patients undergoing MR scans, we analyzed T1 and T2 signal intensities (SI), categorized as low-, iso-, and high SI compared to the surrounding muscle. On enhanced T1WI we evaluated the degree of enhancement (none, mild to moderate, and strong) and the enhancement pattern (homogeneous or heterogeneous). On MR, we evaluated the presence of a nonenhancing low-SI band showing low SI on T2WI without enhancement, and internal signal voids in the tumors.

We investigated the CT and MR predictors for recurrence by dividing the cases into 2 groups (group 1, recurrence or progression; group 2, no recurrence or no treatment).

Finally, we also evaluated diagnostic accuracy of the ''first impression'' formed at the preoperative CT reading in the formal report on CT prior to tissue confirmation.

FDG PET Protocol and Evaluation

FDG PET was obtained using a PET/CT scanner (Discovery PET/CT 690; GE Health Care, USA). ^{18}F-FDG (5.2 MBq/kg body weight) was intravenously injected after fasting for at least 6 hours, followed by PET/CT scanning after 50 minutes. Images were reconstructed using a 3-dimensional ordered subset expectation maximization algorithm. Attenuation corrections were performed using CT attenuation maps. Standardized uptake values (SUV) were evaluated using lean body mass. The maximum standardized uptake values (max-SUVs) of the lesions on FDG PET/CT in 13 patients who had available FDG PET/CT images were calculated.

Histopathological Analysis

Specimens were fixed in formalin, and sections were stained using hematoxylin and eosin stain. The specimens were reviewed by pathologist of soft tissue tumor (JSS). To differential diagnosis, immunohistochemistry was performed in 28 of 47 cases. The immunohistochemical staining for smooth muscle actin (SMA, 1:200, Dako, Denmark), Demin (1:200, Dako, Denmark), CD34 (1:500, Immunotech, Marseille, France), β-Catenin (1: 500, Pharmingen, NJ), Ki-67 labeling index (1:200, Dako) and S100 protein (1: 200, ZYMED, CA) were performed using the Ventana NX automated immunohistochemistry system (Ventana Medical Systems, Tucson, AZ).

Statistical Analysis

Statistical analysis was performed using a commercial statistical software package (SPSS for Windows, version 21.0; SPSS Inc, Chicago, IL) (SSK, not an author, 10 years' experience in medical statistics). Univariate and multivariate logistic regression analysis were used to identify the risk factors for the patients with recurrence or progression. All covariates with a P value < 0.10 in the univariate analysis were included in the multivariate logistic regression analysis. Multivariate logistic regression analysis was used to estimate the P value, odds ratio (OR), and 95% confidence interval (CI). A P value less than 0.05 was considered statistically significant.

RESULTS

Patient Characteristics

Table 1 summarizes the clinical characteristics of the 47 patients. Their median age was 45 (range, 4–96) and their mean age was 44 ± 17-years old. There were more females (n = 30, 63.8%) than males (ratio 1.8:1). The most common symptom was a palpable mass (44.7%) followed by pain (23.4%). Ten patients (21.3%) without symptoms were found incidentally. Almost half of the patients (n = 19, 47.5%) suffered recurrence or progression after treatment (n = 40). The disease-specific survival rate was 100% as of the latest outpatient follow-up.

CT and MR Evaluation

Median long and short tumor diameters were 65 mm (range, 22–126 mm) and 36 mm (range, 9–88 mm), respectively. The most common locations were the chest wall (n = 20, 42.6%) (Figure 2) followed by the supraclavicular area (Figure 3), shoulder or axilla (Figure 4), and mediastinum (Figure 5). Most tumors had well-defined margins (n = 39, 83.0%) (Figure 2) and over half had lobulated contours (n = 31, 66.0%) (Figure 3).

On pre-enhanced CT scans (n = 25), more than half the tumors showed low attenuation (n = 15, 60.0%). Homogeneous enhancement (n = 20, 57.1%) (Figures 2 and 5) was more common than heterogeneous enhancement (n = 15, 42.9%) on post-enhanced CT (n = 35). Among the 23 patients with both pre- and postenhanced CT scans, the degree of enhancement was usually none to mild, with a median value of 24 HU (range, 0–52 HU).

On MR imaging (n = 32), the tumors often showed iso-SI (n = 31, 96.9%) on T1WI and high SI (n = 29, 90.6%) on T2WI. On enhanced MR, strong enhancement (n = 28, 87.5%) was much more common than mild to moderate enhancement, and heterogeneous enhancement (n = 31, 96.9%) was much more common than homogeneous enhancement. Nonenhancing low signal bands were present in 27 patients (84.4%), and internal signal voids were seen in 22 patients (68.8%) (Figures 3 and 5).

The diagnostic accuracy of the ''first impression'' of the MR reports (34.4%) was higher than that of the CT reports (11.1%). On CT, tumors misdiagnosed as desmoid-type fibromatosis of the

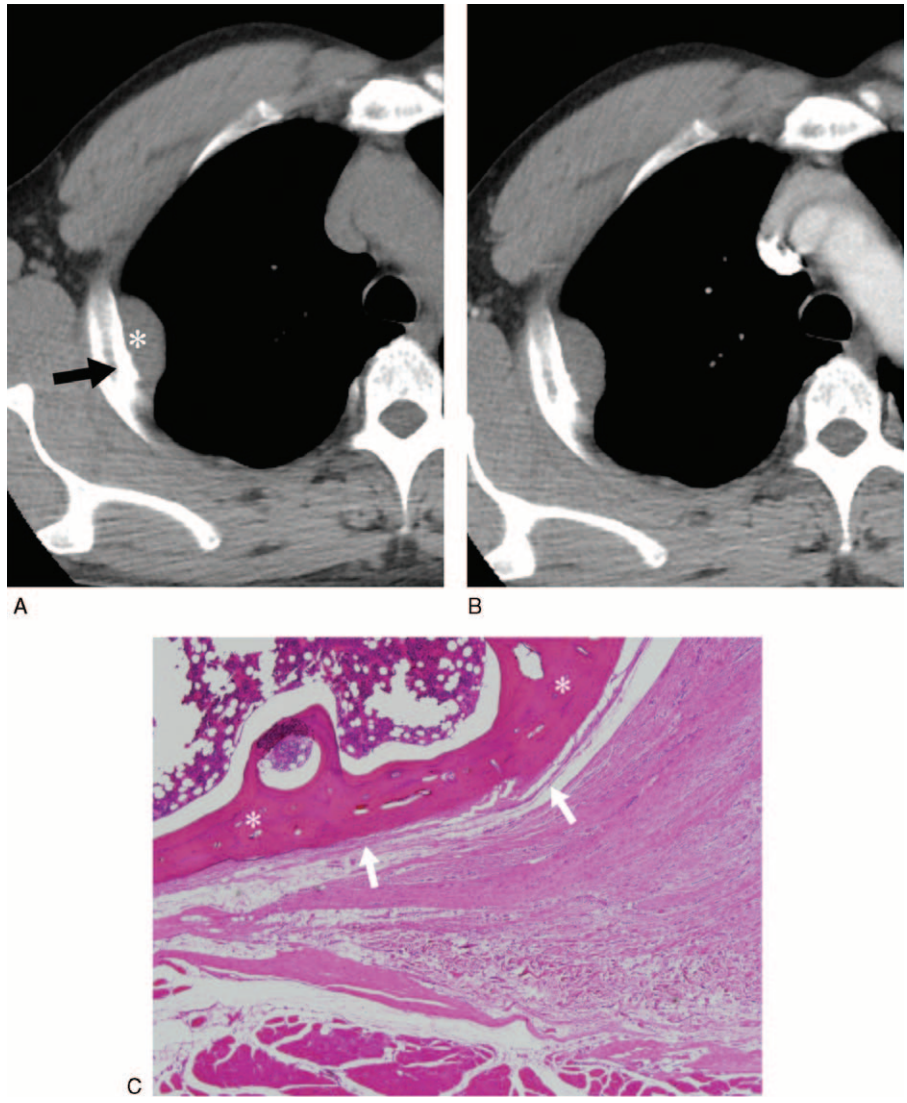

FIGURE 2. A 52-year-old man with desmoid-type fibromatosis in the chest wall without recurrence (Group 2). This was misdiagnosed as a neurogenic tumor based on preoperative CT but as fibromatosis based on preoperative MR. Axial pre- (A) and contrast-enhanced (B) CT axial images (5-mm reconstruction) show a circumscribed, well-defined mass (*) without enhancement in the right chest wall. Note the osteoblastic change of the rib (arrow). FDG PET reveals a hypometabolic mass, with a maximal standardized uptake value of 2.3 (not shown). (C) A mass shows abutting the rib (*) with no evidence of invasion of the cortex of bone and periosteum (arrows, ×40 magnification). CT = computed tomography, MR = magnetic resonance, FDG PET = ^{18}F-fluorodeoxy glucose positron emission tomography.

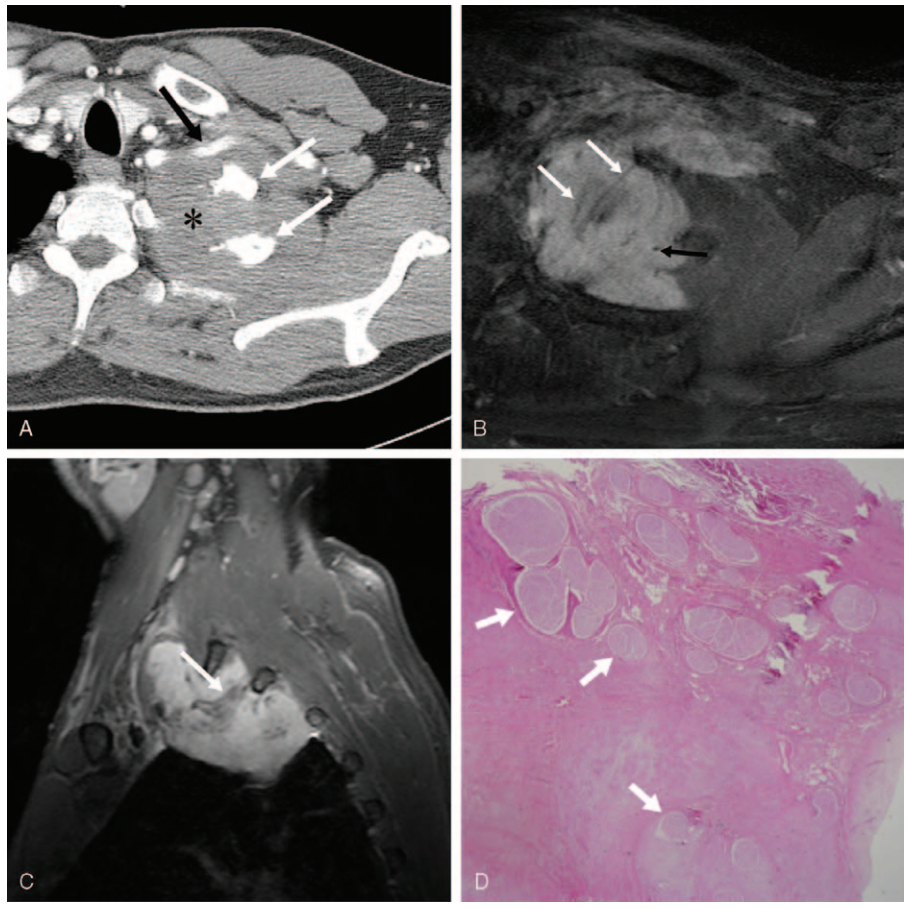

FIGURE 3. A 47-year-old man presented with desmoid-type fibromatosis in the left supraclavicular area with recurrence (Group 1). It was misdiagnosed as a pancoast tumor due to lung cancer and a sarcoma of mesenchymal origin, based on preoperative CT and MR, respectively. (A) The contrast-enhanced axial (A) CT image (5-mm reconstruction) shows a huge, lobulated, partially ill-defined mass in the supraclavicular area (*). Note the osteoblastic change of the first and second ribs (white arrows) and suspicion of involvement of the left subclavian artery (black arrow). Note the strong and heterogeneous enhancement with central areas of nonenhancing low signal bands (white arrows) and internal signal voids (black arrow) on enhanced T1-weighted axial (B) and sagittal (C) images. FDG PET revealed a hypermetabolic mass with a maximal standardized uptake value of 4.1 (not shown). (D) The mass was excised. Pathologically, the mass has infiltrated the brachial plexus, and tumor cells surround the nerve bundles (arrows, ×12.5 magnification). CT = computed tomography, MR = magnetic resonance, FDG PET = ^{18}F-fluorodeoxy glucose positron emission tomography.

thorax were soft tissue sarcomas such as fibrosarcomas (n = 8, 40.0%), neurogenic tumors (n = 5, 25.0%), solitary fibrous tumors of the pleura (n = 4, 20%), and lung cancers (n = 2, 10.0%). On MR, misdiagnoses involved soft tissue sarcomas (n = 3, 50.0%) and neurogenic tumors (n = 2, 33.3%) (Table 2).

FDG PET Evaluation

For the 13 patients with FDG PET scans, the median value of maxSUV was 3.1 (range, 2.0–7.3). The median long axial diameter in the 6 patients with hypometabolic desmoid-type fibromatosis (<2.5 maxSUV) was 41.5 mm (range, 27–90 mm), while the median diameter in the 7 patients with hypermetabolic desmoid-type fibromatosis (>2.5 maxSUV) was 68 mm (range, 35–115 mm) (Table 2).

Histopathological Analysis

The tumor cells were partly positive for SMA in 86.4% (19/22) cases, and β-Catenin in all (17/17) cases with nuclear stain, and negative for CD34, Demin, S100 protein, CD34, supporting the diagnosis of desmoids type fibromatosis. The Ki-67 labeling index showed low proliferative index ranging from 1% to 3%.

Predictors for Tumor Recurrence or Progression

In univariate analysis, Group 1 contained more tumors with partially ill-defined margins than group 2 ($P = 0.043$). There were no significant differences between the 2 groups in other clinical parameters such as age, and radiological parameters such as size, contour, presence of surrounding fat, extra-compartment extension, bone involvement, and neurovascular involvement. Partially ill-defined margin ($P = 0.043$) and extra-compartment extension ($P = 0.084$) were included in the multivariate logistic regression analysis. In multivariable analysis, partially ill-defined margin ($P = 0.043$, OR 0.167, 95% CI 0.029–0.943) was the independent predictor for recurrence or progression (Table 3).

DISCUSSION

Desmoid-type fibromatosis is reported to occur at any age, but to be more common between 10 and 40 years of age, and

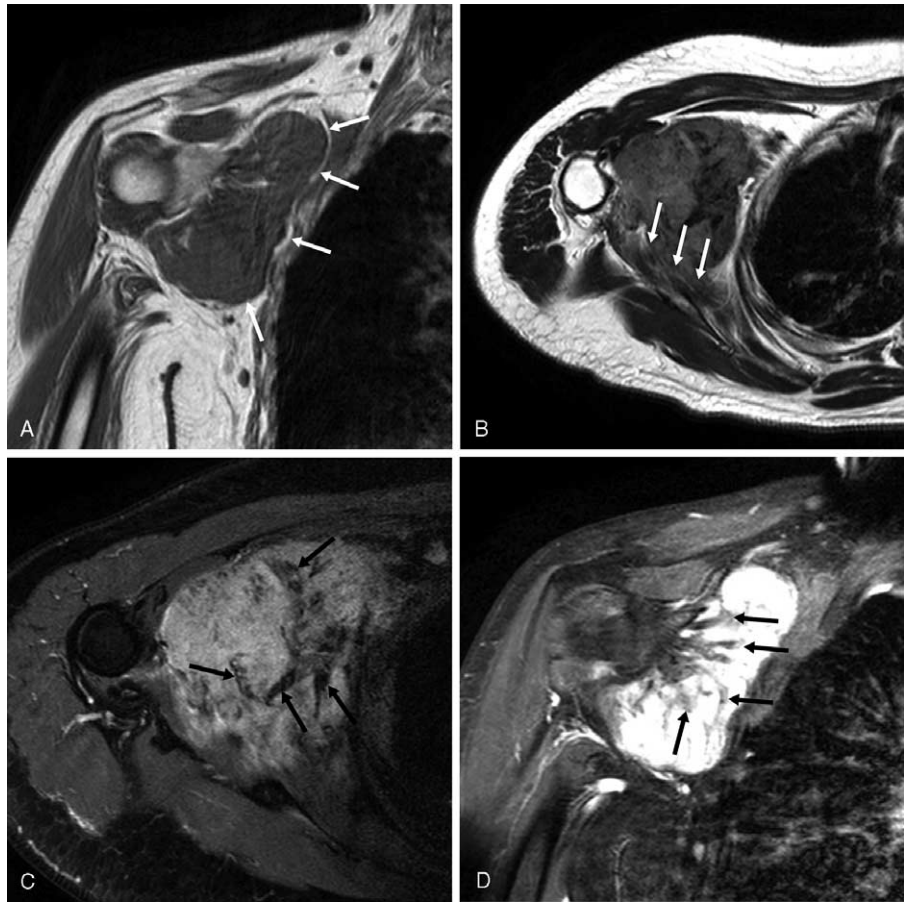

FIGURE 4. A 47-year-old woman with desmoid-type fibromatosis in the right axilla with progression (Group 1). This was misdiagnosed as a sarcoma on preoperative CT but as fibromatosis on preoperative MR. The tumor shows iso-signal intensity on coronal T1-weighted image (A) and high signal intensity on axial T2-weighted image (B). The margin is partially ill-defined (white arrows) on axial T2-weighted image (B). A rim of surrounding fat (white arrows) with high signal intensity is clearly seen on T1-weighted image (A). On enhanced T1-weighted axial (C) and coronal (D) images, the tumor shows strong and heterogeneous enhancement with a central area of nonenhancing low signal bands (black arrows). The maximal standardized uptake value on FDG PET was 2.1 (not shown). CT = computed computed tomography, MR = magnetic resonance, FDG PET = ^{18}F-fluorodeoxy glucose positron emission tomography.

females predominate.[13] In our study, median age was 45 years with a slight female predominance (63.8%), and the most common symptom was a palpable mass. Desmoid-type fibromatosis can occur as part of hereditary syndromes, such as familial adenomatous polyposis, which is often associated with mutations of the adenomatosis polyposis coli gene.[14,15] There was one such case in this study.

Desmoid-type fibromatosis typically has poorly defined margins, infiltrates surrounding soft tissue and skeletal muscle bundles, and is composed of proliferating spindle-shaped, slender, or elongated cells with dense keloid-like collagen stroma on pathology.[2]

In our study, desmoid-type fibromatosis commonly presented as a chest wall mass with well-defined margin and lobulated contour. Like most soft-tissue sarcomas, cross-sectional images showed that it grew as a space-occupying intramuscular lesion, enlarging in a centripetal fashion by pushing rather than infiltrating local structures. Desmoid-type fibromatosis arises from musculo-aponeurotic or fascial structures that are normally surrounded by fat, and that fill the mass as it grows. It typically forms a pseudocapsule as it enlarges by compressing normal tissue and respects fascial boundaries, remaining within a given anatomic compartment until late in its course. With regard to its relationship with surrounding structures, surrounding fat, extra-compartment extension, bone involvement, and neurovascular involvement were common in our cohort. Larger desmoid-type fibromatosis tends to form extra-compartment extension more often that than smaller one.

Compared to primary desmoid-type fibromatosis, recurrent tumors are more invasive and more likely to have ill-defined margins. Lee et al[10] and Liu et al[6] both found that ill-defined margins were more common in cases with recurrence.

In our study, we observed quite frequent bone involvement (42.6%) in the thorax, which appeared as adjacent reactive osteoblastic changes and/or cortical hypertrophy. None of the cases had osteolytic bony lesions. These bony characteristics will be useful in differentiating these tumors from malignant soft tissue sarcoma, metastasis with unknown primary site, or peripheral lung cancer with extra-pulmonary involvement. The evidence of bone involvement is more specific on CT than on MR images.

On CT scans, desmoid-type fibromatosis generally had lower density with homogeneous attenuation and mild enhancement

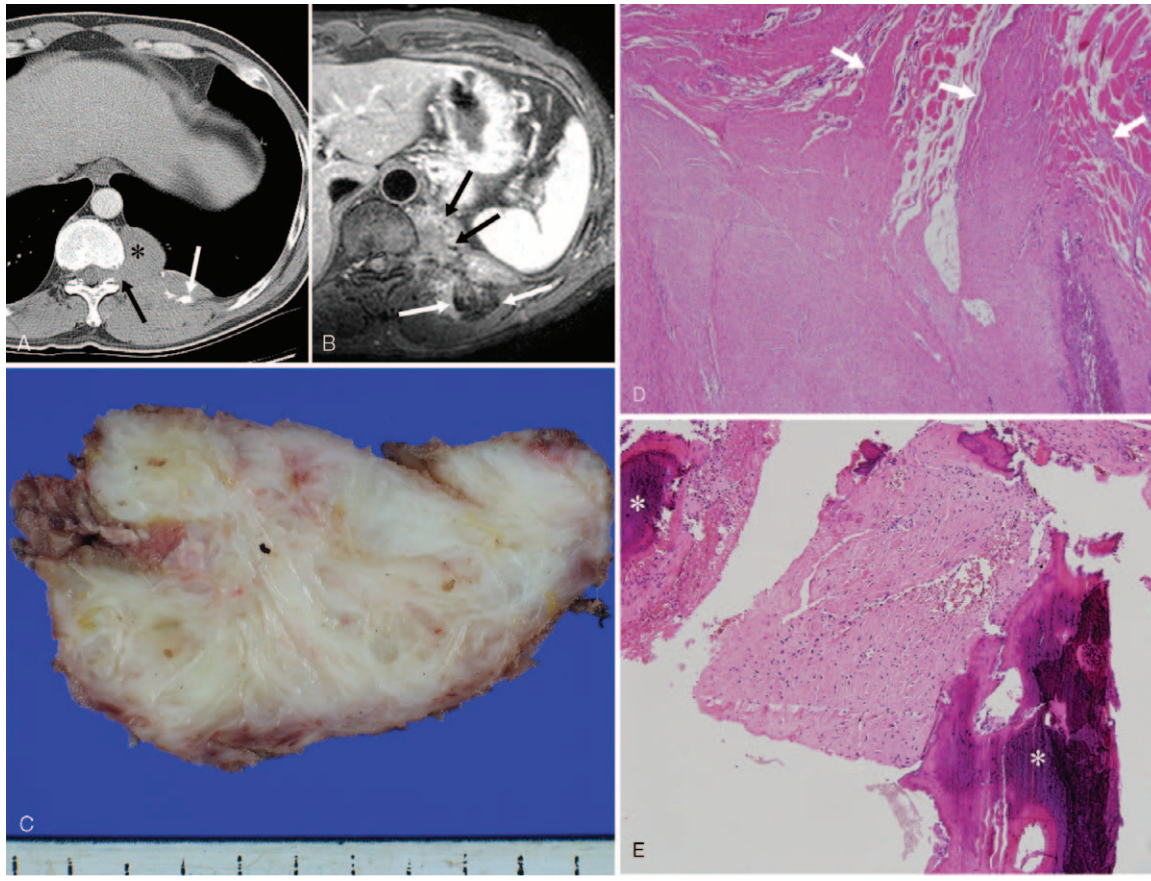

FIGURE 5. A 43-year-old man with desmoid-type fibromatosis in the mediastinum with recurrence (Group 1). This was misdiagnosed as a neurogenic tumor and as fibrosarcoma on preoperative CT and MR, respectively. (A) The contrast-enhanced axial CT image (5-mm reconstruction) shows a lobulated, well-defined mass (*) with mild homogeneous enhancement in the left posterior mediastinum. The difference in Hounsfield units between pre- and postenhancement is 7. Note the osteoblastic change of the rib (white arrow) and the neural foraminal widening (black arrow). (B) The tumor shows strong heterogeneous enhancement on an enhanced T1-weighted image. Note the internal nonenhancing low signal bands (white arrows) and internal signal voids (black arrows). (C) Grossly, an ill-defined irregularly-shaped firm mass is present. The cut surface of the mass glistens, and is whitish gray, coarsely trabeculated and partly myxoid, without hemorrhage and necrosis. (D) Tumor cells infiltrate the chest wall muscle (white arrows, ×40 magnification) and (E) also the marrow space of the rib (*, ×100 magnification). CT = computed tomography, MR = magnetic resonance.

compared to muscle. Internal calcification and necrotic changes were never seen on CT, despite the larger size of the tumors. This characteristic can be helpful for differentiation from soft tissue sarcoma: as the latter increases in size, the blood supply becomes insufficient, and necrosis and cystic degeneration develop.[16]

MR has high soft tissue resolution and is considered the first choice for evaluating the relationship between soft tissue tumors and surrounding structures, such as bone, vessels, and nerves. Typical desmoid-type fibromatosis shows iso-SI on T1WI, high SI on T2WI, and strong heterogeneous enhancement on enhanced T1WI. The heterogeneous enhancement may correspond to varying proportions of myxoid tissue, cellular tissue, and collagenous stroma on pathology.[17] In our study, nonenhancing low signal intensity bands were seen in up to 84.4% of the cases in enhanced T1WI. This characteristic is believed to be due to pathologic change with dense collagenization.[9,18,19] A specific band-like low signal is usually seen in T1WI and T2WI of the tumor without enhancement. This characteristic should be helpful in differential diagnosis of soft tissue sarcoma and neurogenic tumor. In our study, 68.8% of case show internal signal void. According to Oka et al,[20] diffusion-weighted imaging can be helpful in differentiating desmoid-type fibromatosis from malignant soft tissue tumor.

We found that only a few cases showed strong enhancement on CT. However, most cases (87.5%) showed strong enhancement on MR, and we propose that this difference is due to different phases. For CT scans, the interval between contrast administration and scanning is much shorter than for MR scans. As seen in one of our cases, desmoid-type fibromatosis shows gradual enhancement in the delayed phase despite being a hypervascular tumor according to pathology. We believe that dynamic CT scans will be helpful in diagnosis of desmoid-type fibromatosis in future prospective studies.

The accuracy of our diagnosis of desmoid-type fibromatosis on cross-sectional images was very low despite the fact that the study was performed in a tertiary referral center by several expert chest radiologists. The diagnostic accuracy of ''first impressions'' based on MR (34.4%) was higher than that based on CT (11.1%). On both CT and MR, the tumors misdiagnosed as desmoid-type fibromatosis of the thorax were

TABLE 2. CT, MR, and FDG PET Characteristics of the 47 Patients with Desmoid-type Fibromatosis

Imaging Characteristic	Median (Range) or Number (%)
CT and MR characteristic, n = 47	
Size, mm	
Long diameter	65.0 (22–126)
Short diameter	36.0 (9–88)
Location	
Chest wall	20 (42.6)
Supraclavicular	12 (25.5)
Shoulder or axilla	11 (23.4)
Mediastinum	4 (8.5)
Margin	
Well-defined	39 (83.0)
Partially ill-defined	8 (17.0)
Contour	
Lobulated	31 (66.0)
Circumscribed	10 (21.3)
Irregular	6 (12.8)
Rim of surrounding fat	30 (63.8)
Extra-compartment extension	20 (42.6)
Bone involvement	20 (42.6)
Neurovascular involvement	13 (27.7)
CT characteristic, n = 36	
Attenuation relative to muscle on pre-enhanced CT, n = 25	
Low attenuation	15 (60.0)
Iso attenuation	9 (36.0)
High attenuation	1 (4.0)
Heterogeneities on enhanced CT, n = 35	
Homogeneous attenuation	20 (57.1)
Heterogeneous attenuation	15 (42.9)
Attenuation difference, HU using pre- and postenhancement, n = 23	24 (0–52)
MR characteristic, n = 32	
T1WI	
Low SI	1 (3.1)
Iso SI	31 (96.9)
High SI	0 (0.0)
T2WI	
Low SI	0 (0.0)
Iso SI	3 (9.4)
High SI	29 (90.6)
Enhanced T1WI	
None enhancement	0 (0.0)
Mild to moderate	4 (12.5)
Strong	28 (87.5)
Heterogeneity	
Homogeneous SI	1 (3.1)
Heterogeneous SI	31 (96.9)
Non-enhancing low signal intensity band	27 (84.4)
Internal signal void	22 (68.8)
FDG PET Characteristic, n = 13	
maxSUV	3.1 (2.0–7.3)
Long axial diameter, mm	
Hypometabolic tumors (n = 6)	41.5 (27–90)
Hypermetabolic tumors (n = 7)	68 (35–115)

Numbers are number of patients, and numbers in parentheses are percentages or range. FDG PET = ^{18}F-fluorodeoxyglucose positron emission tomography, maxSUV = maximum standardized uptake value, SI = signal intensity.

soft tissue sarcomas such as fibrosarcoma and neurogenic tumor.

Kasper et al[12] found that the median maxSUV on FDG PET was 4.1 (range, 1.0–8.1). We obtained a similar result with a median maxSUV of 3.1 (range, 2.0–7.3). Desmoid-type fibromatosis usually appears moderately hypermetabolic on FDG PET even in large masses, while smaller tumors tended to appear hypometabolic. FDG PET could be useful for evaluating recurrent and progressive tumors.

Surgical excision is recommended as the primary treatment method for desmoid-type fibromatosis.[21,22] In our study, 35 patients underwent surgery. However, in many cases, surgical excision with clear margins is challenging because of the complex anatomic locations and the aggressive growth of desmoid-type fibromatosis. Therefore, many adjuvant treatments such as chemotherapy and radiotherapy have been tried; however, the effects of these treatments are controversial.[23,24] In our study, almost half (n = 19/40, 47.5%) of the tumors recurred at least once, or progressed after treatment. A partially ill-defined margin was the only radiological predictor of future recurrence or progression. Currently, the relationship between recurrence and surgical resection margin is still not well-established. It is worth mentioning that stabilization and spontaneous regression of either primary or recurrent desmoid-type fibromatosis can take place.[25–27] So a ''wait and watch'' policy may be the optimum choice in the management of selected patients.[24] In our cohort, 7 cases were under ''wait and watch,'' of which 1 underwent spontaneous partial regression.

Our study had several limitations. First, it was a retrospective study performed at a single, tertiary referral center, and selection bias was possible in the cohort patients. Second, the diversity of the CT and MR findings prevented them from being categorized according to our usual classification of extra-pulmonary tumor of the thorax, and morphologic evaluation on CT and MR may be subjective. However, we tried to compare radiologic findings between the tumor recurrence or progression and no recurrence or stable disease. The statistical significance was marginal in our study between 2 groups due to the uncommon disease. A larger sample size through multicenter study would be helpful for statistical analysis to compare recurrence and no recurrence groups. Finally, the number of FDG PET studies was relatively small. Nevertheless, the strengths of the study include the large number of patients in a single ethnic group, and providing the detailed descriptions of the CT and MR features, with a focus on the specific inner and

TABLE 3. Univariate and Multivariate Logistic Regression Analysis of the Clinical and Imaging Characteristics as Predictors of Recurrence or Progression in 47 Patients With Desmoid-Type Fibromatosis

			Univariate Analysis	Multivariate Analysis		
Imaging Characteristics	**Group 1 (n = 19) Recurrence (n = 13) Progression (n = 6)**	**Group 2 (n = 28) No Recurrence (n = 21) No Treatment (n = 7)**	***P* Value**	***P* Value**	**OR**	**95% CI**
Age (median, range, year)	45 (23–55)	47 (4–96)	0.446			
Size (median, range, mm)						
Long diameter	68.0 (40–126)	63.0 (22–115)	0.371			
Short diameter	40.0 (20–65)	35.0 (9–88)	0.907			
Margin			0.043	0.043	0.167	0.029–0.943
Well-defined	13 (68.4)	26 (92.9)				
Partially ill-defined	6 (31.6)	2 (7.1)				
Contour			0.706			
Lobulated	13 (68.4)	18 (64.3)				
Circumscribed	3 (15.8)	7 (25.0)				
Irregular	3 (15.8)	3 (10.7)				
Rim of surrounding fat	13 (68.4)	17 (60.7)	0.590			
Extra-compartment extension	11 (57.9)	9 (32.1)	0.084			
Bone involvement	10 (52.6)	10 (35.7)	0.252			
Neurovascular involvement	7 (36.8)	7 (25.0)	0.386			

CI = confidence interval, OR = odds ratio. Values are the number of patients, and numbers in parentheses are percentages or range.

outer morphology of the tumor. We also tried to clarify the FDG PET findings of the tumor.

In summary, desmoid-type fibromatosis should be considered especially in middle-aged women with a palpable mass with CT and MR features pointing to an extra-pulmonary tumor, especially in the chest wall, with a well-defined margin, lobulated contour, and presence of a rim of surrounding fat on cross-sectional images. Desmoid-type fibromatosis shows mild and homogeneous enhancement on CT, strong heterogeneous enhancement with nonenhancing lower SI bands or signal void on enhanced MR, and moderately hypermetabolic on FDG PET. Partially ill-defined margin of the tumor is the only predictor of recurrence or progression on preoperative cross-sectional images. Observation of the margin of the tumor on initial presentation and on recurrence is important for the radiologists to estimate the likelihood of recurrence.

CONCLUSIONS

Knowledge regarding the radiological findings of desmoid-type fibromatosis on CT, MR, and FDG PET will help make a correct diagnosis. Tumors with partially ill-defined margins have a tendency to recur or progress.

REFERENCES

1. Weiss SW, Goldblum JR, Flope AL. Enzinger and Weiss's Soft Tissue Tumors: Expert Consults. 6th ed. Philadelphia: Saunders Elsevier; 2014:288–293.
2. Fletcher CD, Unni KK, Mertens F. Pathology and Genetics of Tumours of Soft Tissue and Bone. Lyon: IARC Press; 2002:83.
3. Hosalkar HS, Torbert JT, Fox EJ, et al. Musculoskeletal desmoid tumors. *J Am Acad Orthop Surg*. 2008;16:188–198.
4. Nuyttens JJ, Rust PF, Thomas CR Jr et al. Surgery versus radiation therapy for patients with aggressive fibromatosis or desmoid tumors: a comparative review of 22 articles. *Cancer*. 2000;88:1517–1523.
5. Janinis J, Patriki M, Vini L, et al. The pharmacological treatment of aggressive fibromatosis: a systematic review. *Ann Oncol*. 2003;14: 181–190.
6. Liu QY, Chen JY, Liang BL, et al. Imaging manifestations and pathologic features of soft tissue desmoid-type fibromatosis. *Ai Zheng*. 2008;27:1287–1292.
7. Kabiri EH, Al Aziz S, El Maslout A, et al. Desmoid tumors of the chest wall. *Eur J Cardiothorac Surg*. 2001;19:580–583.
8. Zehani-Kassar A, Ayadi-Kaddour A, Marghli A, et al. Desmoid-type chest wall fibromatosis. A six cases series. *Orthop Traumatol Surg Res*. 2011;97:102–107.
9. Rai AT, Nguyen TP, Hogg JP, et al. Aggressive fibromatosis of the neck in a patient with Gardner's syndrome. *Neuroradiology*. 2001;43:650–652.
10. Lee JC, Thomas JM, Phillips S, et al. Aggressive fibromatosis: MRI features with pathologic correlation. *AJR Am J Roentgenol*. 2006;186:247–254.
11. Mori T, Yamada T, Ohba Y, et al. A case of desmoid-type fibromatosis arising after thoracotomy for lung cancer with a review of the english and Japanese literature. *Ann Thorac Cardiovasc Surg*. 2014;20(Suppl):465–469.
12. Kasper B, Dimitrakopoulou-Strauss A, Strauss LG, et al. Positron emission tomography in patients with aggressive fibromatosis/ desmoid tumours undergoing therapy with imatinib. *Eur J Nucl Med Mol Imaging*. 2010;37:1876–1882.
13. Shields CJ, Winter DC, Kirwan WO, et al. Desmoid tumours. *Eur J Surg Oncol*. 2001;27:701–706.
14. Clark SK, Phillips RK. Desmoids in familial adenomatous polyposis. *Br J Surg*. 1996;83:1494–1504.
15. Wallis YL, Morton DG, McKeown CM, et al. Molecular analysis of the APC gene in 205 families: extended genotype-phenotype correlations in FAP and evidence for the role of APC amino acid changes in colorectal cancer predisposition. *J Med Genet*. 1999;36:14–20.

16. Peabody TD, Simon MA. Principles of staging of soft-tissue sarcomas. *Clin Orthop Relat Res.* 1993:19–31.
17. Romero JA, Kim EE, Kim CG, et al. Different biologic features of desmoid tumors in adult and juvenile patients: MR demonstration. *J Comput Assist Tomogr.* 1995;19:782–787.
18. Sundaram M, McGuire MH, Schajowicz F. Soft-tissue masses: histologic basis for decreased signal (short T2) on T2-weighted MR images. *AJR Am J Roentgenol.* 1987;148:1247–1250.
19. Shinagare AB, Ramaiya NH, Jagannathan JP, et al. A to Z of desmoid tumors. *AJR Am J Roentgenol.* 2011;197:W1008–W1014.
20. Oka K, Yakushiji T, Sato H, et al. Usefulness of diffusion-weighted imaging for differentiating between desmoid tumors and malignant soft tissue tumors. *J Magn Reson Imaging.* 2011;33:189–193.
21. Merchant NB, Lewis JJ, Woodruff JM, et al. Extremity and trunk desmoid tumors: a multifactorial analysis of outcome. *Cancer.* 1999;86:2045–2052.
22. Huang K, Fu H, Shi YQ, et al. Prognostic factors for extra-abdominal and abdominal wall desmoids: a 20-year experience at a single institution. *J Surg Oncol.* 2009;100:563–569.
23. Hoos A, Lewis JJ, Urist MJ, et al. Desmoid tumors of the head and neck—a clinical study of a rare entity. *Head Neck.* 2000;22:814–821.
24. Joglekar SB, Rose PS, Sim F, et al. Current perspectives on desmoid tumors: the mayo clinic approach. *Cancers (Basel).* 2011;3:3143–3155.
25. Fiore M, Rimareix F, Mariani L, et al. Desmoid-type fibromatosis: a front-line conservative approach to select patients for surgical treatment. *Ann Surg Oncol.* 2009;16:2587–2593.
26. Tsukiyama I, Kakehi M, Yanagawa S, et al. Extra-abdominal desmoid tumor – report of a case. *Gan No Rinsho.* 1984;30:1693–1699.
27. Barbier O, Anract P, Pluot E, et al. Primary or recurring extra-abdominal desmoid fibromatosis: assessment of treatment by observation only. *Orthop Traumatol Surg Res.* 2010;96:884–889.